Journal of
Renewable Energy Research and Applications (RERA)

Vol. 5, No 2, 2024, 243-258 *DOI: 10.22044/rera.2023.13426.1239*

Development of a New Method in Exergy Analysis of a CSP Plant

M. Akbari Vakilabadi[1*], S. Nikbakht Naserabad[2], A. Binesh[1]

1. Faculty of Naval Aviation, Malek Ashtar University of technology, Iran.
2. Energy Engineering Department, Faculty of Gas and Petroleum, Yasouj University, Gachsaran, Iran.

Received Date 31 June 2023; Revised Date 13 July 2023; Accepte Date 24 August 2023
**Corresponding author: M_akbari@mut.ac.ir (M. Akbari Vakilabadi)*

Abstract
In this work, it is determined exactly how much of the loss of exergy in a specify component is concerning the own component and how much of the exergy loss is due to the effects of the rest of the components on that component. In this new method of exergy analysis, at first, the exergy loss in a component is classified as avoid./unavoid categories. With this classification, it is possible to understand what quantity of the exergy loss of a component is eliminated by optimizing that component, and how much of the exergy dissipation can never be eliminated, and is related to the nature of the component. In the next classification, by categorizing the exergy loss into endo./exo., we can find out how much of the exergy destruction is due to the non-optimality of other components, and has nothing to do with the component itself. Finally, the categories are divided into avoid-endo, unavoid-endo, avoid-exo, and avoid-enxo. By performing this new method, the results demonstrate that the highest exergy destruction (1.976 MW) happens in the evaporator, 68% of which is unavoid-endo. exergy loss. The highest avoid. exergy loss relates to low pressure turbine (0.5791 MW). It is shown that optimizing of the surrounding components of deaerator, economizers, and evaporators has a greater effect on decreasing the exergy dissipation of these own components, and the most avoid. exergy destruction is in heat exchangers, pumps, condensers, turbines, expansion valves, reheaters, and superheaters.

Keywords: *Advanced exergy analysis, Solar power plant, Endo./Exo. exergy loss, avoid./Unavoid. exergy loss.*

1. Introduction

In the recent years, many researchers have done a lot of research works on thermal power plants, and have always been looking for a way to improve and develop the cycle used and have done a lot of thermodynamic analysis in this case [1]. One of the analyses that have been used is the traditional exergy analysis. Analysis of exergy is actually identifying and specifying the useful amount of energy to perform a thermodynamic process and also calculating exergy losses in the desired process. Traditional analysis of exergy is not able to determine whether this destruction is due to irreversibility in the own component or due to irreversibility in other components and how much this destruction can be reduced. In the recent years, a new method has been applied to different energy cycles, which is known as advanced exergy analysis, which is very necessary for the improvement and development of the steam power cycle and for thermos-economic analysis. In this new method, it is clear that to improve the cycle efficiency, it is important to know which component to focus more on and how much progress and existing technology can be useful in reducing destruction or exergy losses. In order to reduce environmental pollutants, renewable energy has grown significantly. Greatest challenge of using renewable energies is their low efficiency. For this reason, most of the studies are aimed at increasing the efficiency of using renewable energy. In 2020, Akbari *et al*. performed analysis of exergy in a CSP plant. They concluded that the maximum exergy loss occurs in solar collectors and the lowest loss is in the turbine[2]. In two other studies, they enhanced the productivity of the CSP plant by recycling the effluent from a solar thermal power plant [3, 4].
Saeidi *et al*. studied analysis of exergy in a co-generation plant. They concluded that by returning the heat in the effluent, it is possible to start an organic Rankine cycle and increase the power plant efficiency [5]. M A Vakilabadi *et al*. investigated the hydrodynamic behavior of particles in biomass combustion. They modeled

the forces on the particles, and concluded that the thermophoretic force has a significant effect on the location of the flame [6, 7]. Koroglu and Sogut performed exergy analysis of a marine facility. In this study, they demonstrated that the most Avoid. exergy loss happens in the boiler [8]. Mohamed Elhelw *et al*. conducted analysis of exergy for a thermal plant in two different modes [9]. L. Cai *et al*. studied advanced exergy analysis of a LNG oxy-fuel CSP plant. By adding oxy-fuel combustion to the power plant, they concluded that 81.68% of exergy loss in this system is Avoid.[10]. Yan Cao et al investigated advanced exergy analysis for a solar power generation cycle. They concluded that the exergy efficiency is 7.011%, which is 8.973% Unavoid.[11]. L. Anetor *et al*. performed traditional and advanced analysis of exergy for a 750 kW power plant. They concluded that to enhance the efficiency of the condenser and boiler, it is better to reduce their Endo. Avoid. exergy losses [12]. Obieda R. Altarawneh *et al*. carried out exergy and energy analysis for a CCPP in Jordan. They concluded that thermal contrast between the burners and the surrounding atmosphere is the main reason for exergy loss in the boiler, which reduces the efficiency of the power plant [12]. AliBasem *et al*. studied energy and exergy analysis of a CSP. Based on their finding, it can be stated that the highest energy loss is 2172.81 W and the maximum exergy loss is 3650.94 W[14]. Yiping Dai et al researched exergy analysis for an IGCC of ejector refrigeration and Rankine power. In this study, a combined cycle simultaneously produces power and acts as a refrigerator. They concluded the most exergy loss is in the boiler and then in the ejector, and turbine inlet pressurehas the greatest effect on turbine output power and combined cycle exergy efficiency [15]. Montazerinejad *et al*. performed advanced analysis of exergy for a fuel cell with energy storage tank. At first, by performing exergy analysis, their finding indicated that the maximum exergy loss is in the PEMFC stack. Also they found that based on advanced analysis of exergy for all components except compressor and condenser, the avoid. exergy loss portion is more than the unavoid portion. The most exo and endo exergy losses occur in compressor and PEMFC, respectively [16]. Mengting Song et al studied advanced exergy analysis for a fuel cell. Their results showed that Solid oxide fuel cell has great potential for energy storage [17].

Yasin Şöhret *et al*. analyzed the gas turbine engine of an aircraft using advanced exergy analysis and identified different parts of exergy loss. They showed that 81.83% of the exergy losses are Endo. [18]. In 2023, Juejing Sheng *et al*. studied advanced analysis of exergy for a hydrocarbon processing facility. Their results demonstrate the exergy loss in compressors is as endo. irreversibility and exergy loss in coolers can be decreased by enhancing other plant components [19]. Advanced exergy analysis for a compressed air energy storage system is performed by YingnanTian *et al*. They concluded that Endo. exergy dissipation of components is more than Exo. exergy dissipation[20]. Abid Ustaoglu *et al*. performed advanced analysis of exergy for a waste incinerator system. In this research work, it has been shown that the primary component to improve exergy losses is turbine, which has the maximum portion of the avoid. Part [21]. Xiaohui Zhong *et al*. performed traditional and advanced analysis of exergy for a renewable energy system. In this research, they concluded that 87.32% of the exergy loss in the compressor is as endo. exergy loss and it is reduced by improving the parameters of the internal design of the compressor [21]. M.F. Ezzat *et al*. used exergy analysis for a power plant with two power sources and showed that the exergy efficiency of this power plant is 50.66% [23]. Hui Yan *et al*. performed an exergy analysis for a coal-solar combined power plant. They concluded that when the solar radiation step is reduced from 700 to 400 W/m^2, the solar exergy to power efficiency increases from 32.62% to 57.25% [24]. Joaquín Zueco and colleagues performed an exergy analysis of a thermal power plant with different fuels such as biodiesel. they investigated the impact of chemical separation of combustion products on exergy efficiency. They concluded that the use of fuels with simple molecular structure reduces exergy destruction [25]. A. Kumar performed an exergy analysis of a 250 kW power plant. They found that the exergy efficiency of the power plant is 34.75% [26]. Zhang et al. conducted thermodynamic analysis of steam recovery system in a CSP power plant in two separate studies. They concluded that exergy recovery can be increased by increasing the initial steam pressure [27, 28]. Yongliang Zhao *et al*. studied advanced exergy analysis for an electricity storage system. They concluded that the maximum avoidable exergy loss occurs in the recuperator [29].

In this research work, advanced analysis of exergy is done for a CSP plant with a capacity of 10 MW. First, by separating the total exergy loss into Avoid./Unavoid., those types of losses that can be eliminated by optimizing the system are

identified. Then by dividing the exergy losses into Endo./Exo., it is determined that the reduction of exergy losses occurs by optimizing the own component or by optimizing other components. Finally, by categorizing exergy losses into Avoid. Endo., Avoid. Exo., Avoidable Endo. and Avoid. Exo., it is determined how much the contribution of each component is in increasing the productivity of the whole cycle.

2. Advanced exergy analysis

In energy analysis, the sustainability of energy in a cycle is investigated, but exergy analysis determines the amount of useful energy that is wasted in a cycle and calculates the contribution of each component in overall exergy losses [30, 31]. The traditional exergy analysis is not a practical way to increase cycle efficiency, because in this analysis, it only tells us the amount of exergy losses in each component in general and is not able to divide the exergy losses into avoid./unavoid. exergy destruction for each component.

In the conventional analysis of exergy, there is no discussion about whether these irreversibilities are caused by the component itself or other components, as well as how much of these irreversibilities can be eliminated and how much cannot be eliminated. In the new method of exergy analysis (advanced exergy analysis), thermodynamic efficiency, cost and ecological consequences are divided into unavoid./avoid. and exo./endo. in each of the system components. In addition, the combination of these, i.e. Endo./Exo. Avoid. and Endo./Exo. Unavoid. is also done. Examining them can help to improve the thermodynamic performance of components. This valuable information cannot be obtained from conventional exergy analysis.

Exo. and Endo. components of exergy losses

Endo. exergy loss in a component is a part of exergy that is obtained in the case that all other components work ideally. Exo. exergy loss has a variable value that is obtained from the difference between total loss and endo. loss and is related to irreversibility in other components.

thermodynamic cycle ($\dot{E}_{D,K}$) is divided from one point of view into two portions, which are endo. part ($\dot{E}_{D,K}^{EN}$) and exo. part ($\dot{E}_{D,K}^{Ex}$), which can be written:

$$\dot{\mathbf{E}}_{\mathbf{D,K}} = \dot{\mathbf{E}}_{\mathbf{D,K}}^{\mathbf{EN}} + \dot{\mathbf{E}}_{\mathbf{D,K}}^{\mathbf{Ex}} \quad (1)$$

In the above relationship, the exo. part is related to the entering flow rate to the component from the rest of the components, and the endo. part is related to the entropy production in the component itself. The information obtained from this division helps the researchers to identify the effect of other components on the exergy destruction of the desired component and to know how much of this exergy loss is attributed by the own component.

The endo. exergy loss of the K component is obtained from analysis of compound cycles. A compound cycle is an ideal cycle that exhibits K component irreversibilities. The count of compound cycles that is formed is the same as the quantity of components in the cycle. The mass flow also changes according to the changes in cycle conditions. Thus for the K-th component, by finding the endo. exergy destruction and having the exergy loss, the exo. exergy loss is calculated:

$$\dot{\mathbf{E}}_{\mathbf{D,K}}^{\mathbf{Ex}} = \dot{\mathbf{E}}_{\mathbf{D,K}} - \dot{\mathbf{E}}_{\mathbf{D,K}}^{\mathbf{EN}} \quad (2)$$

2.2. Avoid. and unavoid. components of exergy losses

Avoid. exergy loss is the potential required to enhance each component. This type of exergy loss is considered in the enhancement process. Its total value is essential in advanced exergy analysis. Because its value briefly expresses all the information about this method and the significance of enhancing each component and the whole cycle. Unavoid. exergy dissipation results are the exergy percentage that is unable to be prevented with existing techniques and economic considerations.

In new method of exergy analysis, the exergy dissipation in K component can be separated into two portions: the Avoid. part ($\dot{E}_{D,K}^{AV}$) and the Unavoid. part ($\dot{E}_{D,K}^{UN}$), which can be written:

$$\dot{\mathbf{E}}_{\mathbf{D,K}} = \dot{\mathbf{E}}_{\mathbf{D,K}}^{\mathbf{AV}} + \dot{\mathbf{E}}_{\mathbf{D,K}}^{\mathbf{UN}} \quad (3)$$

To divide exergy loss into Avoid. and Unavoid. parts, it is vital to develop a cycle where merely unavoid. exergy loss occurs in components. The unavoid. portion of exergy loss in components is achieved using this cycle. The mass flow rate changes as the cycle conditions are changed. In this way, by having the unavoid. portion of exergy loss and the exergy dissipation of kth component, the avoid. exergy loss can be calculated:

$$\dot{\mathbf{E}}_{\mathbf{D,K}}^{\mathbf{AV}} = \dot{\mathbf{E}}_{\mathbf{D,K}} - \dot{\mathbf{E}}_{\mathbf{D,K}}^{\mathbf{UN}} \quad (4)$$

2.3. Combination of Unavoid., Avoid., Exo., and Endo. components of exergy destruction

Using a suitable method, it is possible to obtain Endo. Unavoid. exergy loss of each component.

To calculate the endo.unavoid. part of exergy dissipation of a component in a steam cycle, the hybrid cycle with Unavoid. irreversibility is formed. After calculating the endo. unavoid. exergy loss, it is possible to obtain exo. unavoid. exergy loss, endo. avoid. exergy loss and exo. avoid. exergy loss [32].

$$\dot{\mathbf{E}}_{\mathbf{D,K}}^{\mathbf{UN,EX}} = \dot{\mathbf{E}}_{\mathbf{D,K}}^{\mathbf{UN}} - \dot{\mathbf{E}}_{\mathbf{D,K}}^{\mathbf{UN,AV}} \quad (5)$$

$$\dot{\mathbf{E}}_{\mathbf{D,K}}^{\mathbf{AV,EN}} = \dot{\mathbf{E}}_{\mathbf{D,K}}^{\mathbf{EN}} - \dot{\mathbf{E}}_{\mathbf{D,K}}^{\mathbf{UN,EN}} \quad (6)$$

$$\dot{\mathbf{E}}_{\mathbf{D,K}}^{\mathbf{AV,EX}} = \dot{\mathbf{E}}_{\mathbf{D,K}}^{\mathbf{AV}} - \dot{\mathbf{E}}_{\mathbf{D,K}}^{\mathbf{AV,EN}} \quad (7)$$

Advanced analysis of exergy for a cycle

In the advanced analysis of exergy, an energy system containing three segments is considered as shown in figure 1.

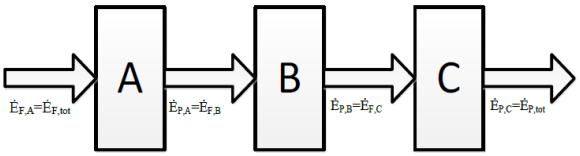

Figure 1. Energy system with three segments.

It is assumed that input A is the input of the whole system, input B is the output of A, input C is the output of B, and output C is the output of the whole system. The efficiency of these components are ϵ_A, ϵ_B and ϵ_C, respectively. To find the amount of endo. exergy loss of each segment, it is enough to take the rest of the components as an ideal and consider only the desired component with real efficiency. Now, if this amount is subtracted from the total exergy destruction, the amount of Exo. exergy destruction is obtained. Below are the relationships related to the calculation of the exo. and endo. value of each of the species A, B and C.

For component C:

$$\dot{\mathbf{E}}_{\mathbf{D,C}}^{\mathbf{EN}} = \dot{\mathbf{E}}_{\mathbf{D,C}} = \dot{\mathbf{E}}_{\mathbf{P,C}}\left(\frac{\mathbf{1}}{\boldsymbol{\epsilon}_{\mathbf{C}}} - \mathbf{1}\right) = \dot{\mathbf{E}}_{\mathbf{P,tot}}\left(\frac{\mathbf{1}}{\boldsymbol{\epsilon}_{\mathbf{C}}} - \mathbf{1}\right) \quad (8)$$

$$\dot{\mathbf{E}}_{\mathbf{D,C}}^{\mathbf{EX}} = \mathbf{0} \quad (9)$$

For component B:

$$\dot{\mathbf{E}}_{\mathbf{D,B}} = \frac{\dot{\mathbf{E}}_{\mathbf{P,tot}}}{\boldsymbol{\epsilon}_{\mathbf{C}}}\left(\frac{\mathbf{1}}{\boldsymbol{\epsilon}_{\mathbf{B}}} - \mathbf{1}\right) \quad (10)$$

$$\dot{\mathbf{E}}_{\mathbf{D,B}}^{\mathbf{EN}} = \dot{\mathbf{E}}_{\mathbf{P,tot}}\left(\frac{\mathbf{1}}{\boldsymbol{\epsilon}_{\mathbf{B}}} - \mathbf{1}\right) \quad (11)$$

$$\dot{\mathbf{E}}_{\mathbf{D,B}}^{\mathbf{EX}} = \dot{\mathbf{E}}_{\mathbf{P,tot}}\left(\frac{\mathbf{1}}{\boldsymbol{\epsilon}_{\mathbf{B}}} - \mathbf{1}\right)\left(\frac{\mathbf{1}}{\boldsymbol{\epsilon}_{\mathbf{C}}} - \mathbf{1}\right) \quad (12)$$

For component A:

$$\dot{\mathbf{E}}_{\mathbf{D,A}} = \frac{\dot{\mathbf{E}}_{\mathbf{P,tot}}}{\boldsymbol{\epsilon}_{\mathbf{B}}\boldsymbol{\epsilon}_{\mathbf{C}}}\left(\frac{\mathbf{1}}{\boldsymbol{\epsilon}_{\mathbf{A}}} - \mathbf{1}\right) \quad (13)$$

$$\dot{\mathbf{E}}_{\mathbf{D,B}}^{\mathbf{EN}} = \dot{\mathbf{E}}_{\mathbf{P,tot}}\left(\frac{\mathbf{1}}{\boldsymbol{\epsilon}_{\mathbf{A}}} - \mathbf{1}\right) \quad (14)$$

$$\dot{\mathbf{E}}_{\mathbf{D,B}}^{\mathbf{EX}} = \frac{\dot{\mathbf{E}}_{\mathbf{P,tot}}}{\boldsymbol{\epsilon}_{\mathbf{B}}\boldsymbol{\epsilon}_{\mathbf{C}}}\left(\frac{\mathbf{1}}{\boldsymbol{\epsilon}_{\mathbf{A}}} - \mathbf{1}\right)\left(\frac{\mathbf{1}}{\boldsymbol{\epsilon}_{\mathbf{B}}\boldsymbol{\epsilon}_{\mathbf{C}}} - \mathbf{1}\right) \quad (15)$$

To obtain the unavoid. exergy loss, the efficiencies related to the Unavoid. part should be used. The Unavoid. value can be theoretically obtained from the following relations.

$$\dot{\mathbf{E}}_{\mathbf{D,tot}}^{\mathbf{UN}} = \dot{\mathbf{E}}_{\mathbf{D,A}}^{\mathbf{UN}} + \dot{\mathbf{E}}_{\mathbf{D,B}}^{\mathbf{UN}} + \dot{\mathbf{E}}_{\mathbf{D,C}}^{\mathbf{UN}} = \dot{\mathbf{E}}_{\mathbf{P,tot}}\left[\left(\frac{1}{\epsilon_{\mathbf{C}}^{\mathbf{UN}}\epsilon_{\mathbf{B}}^{\mathbf{UN}}}\left(\frac{1}{\epsilon_{\mathbf{A}}^{\mathbf{UN}}} - 1\right)\right) + \frac{1}{\epsilon_{\mathbf{C}}^{\mathbf{UN}}}\left(\frac{1}{\epsilon_{\mathbf{B}}^{\mathbf{UN}}} - 1\right) + \left(\frac{1}{\epsilon_{\mathbf{B}}^{\mathbf{UN}}} - 1\right)\right] \quad (16)$$

$$\dot{\mathbf{E}}_{\mathbf{D,tot}}^{\mathbf{AV}} = \dot{\mathbf{E}}_{\mathbf{D,tot}} - \dot{\mathbf{E}}_{\mathbf{D,tot}}^{\mathbf{UN}} = \left(\dot{\mathbf{E}}_{\mathbf{D,A}} - \dot{\mathbf{E}}_{\mathbf{D,A}}^{\mathbf{UN}}\right) + \left(\dot{\mathbf{E}}_{\mathbf{D,B}} - \dot{\mathbf{E}}_{\mathbf{D,B}}^{\mathbf{UN}}\right) + \left(\dot{\mathbf{E}}_{\mathbf{D,C}} - \dot{\mathbf{E}}_{\mathbf{D,C}}^{\mathbf{UN}}\right) \quad (17)$$

All the relationships mentioned in this section are very useful in the theoretical calculation of unavoid., avoid., exo., and endo. parts.

To separate exergy destruction into avoid./unavoid. and endo./exo. parts, the first step is to define the ideal cycle. The general principle in the ideal cycle is that the exergy loss in each component is zero. Therefore, the assumptions are as follow [32].

1. In a heat exchanger with fluid agents that have different heat capacity rates $\Delta T_{min} = 0$ thus $\dot{E}_{D,k}^{th} = min.$
2. In expansion valves $s_1 = s_2$.
3. The process of steam valve is irreversible, and cannot be explained as an ideal process.
4. The mass flow rate changes according to the changed cycle conditions. That is $\dot{m}_{real} = \dot{m}_{th}$.

The compound cycle depicts the ideal cycle with irreversibility only in the desired component. For example, hybrid cycle for the turbine, irreversibility is zero or minimal in all components and there is irreversibility only for the turbine. The total count of compound cycles that must to produce for analysis is the same as the cycle components count. The compound cycles of the cycle members are given in the table 1.

Table 1. Compound cycles of power plant cycle components.

Power plant cycle components	cycle
Pump1	1T,2T,3T,4H,5T,6T,7T,8T,9T,10T,11T,12T,13T,14T
Economizer and Boiler	1T,2T,3T,4H*,5R,6R,7R,8H*,9H,10H**,11T,12H***,13T,14T
Super heater and Re-heater	1T,2T,3T,4H*,5R,6R,7R,8R,9R,10H*,11T,12H**,13T,14T
High pressure turbine	1T,2T,3T,4T,5T,6T,7T,8H,9T,10T,11T,12T,13T,14T
Low pressure turbine	1T,2T,3T,4T,5T,6T,7T,8T,9T,10H,11T,12H,13T,14T
Condenser	1R,2H*,3T,4T,5T,6T,7T,8T,9T,10H**,11T,12T,13T,14T
Pump2	1T,2H,3T,4T,5T,6T,7T,8T,9T,10T,11T,12T,13T,14T
Expansion valve	1T,2T,3T,4T,5T,6T,7T,8T,9T,10T,11H,12T,13T,14T
Heat Exchanger	1T,2T,3T,4T,5T,6T,7T,8T,9T,10T,11T,12H*,13R, 14H*
Pump3	1T,2T,3T,4T,5T,6T,7T,8T,9T,10T,11T,12T,13T,14H
Deaerator	1T,2H**,3R,4H**,5T,6T,7T,8T,9T,10T,11H*,12T,13T,14H**

A cycle with unavoid. exergy loss is based on the real cycle, but it should be irreversible with unavoid. temperature difference in the H.E, unavoid. exergy loss efficiency in the turbine and pump, and the process of steam valve should be considered.

Due to the fact that the cycle examined in this study does not have combustion, therefore, the simple vapor condensation refrigeration cycle shown schematically in figure 2 has been chosen as a validation sample of the method.

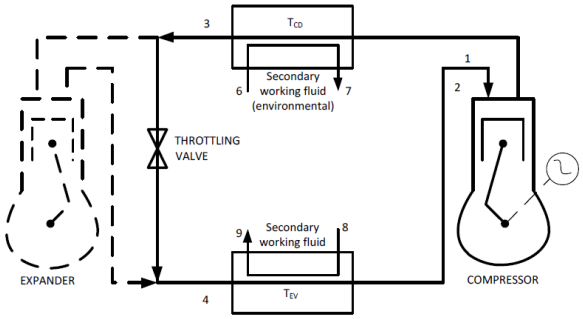

Figure 2. Simple steam compression refrigeration cycle [32].

The cycle examined in this study has many components, and it is actually very complicated to draw the T-S graph for hybrid and ideal cycles simultaneously. For the refrigeration cycle, the T-S graph corresponding to the ideal cycle (with the subscript T), the real cycle (with the subscript R) and the real cycle with Unavoid. irreversibility (with the subscript RU) in figure 3 and the T-S diagram for the real cycle, the ideal cycle and the hybrid cycle for all components is presented in figure 4.

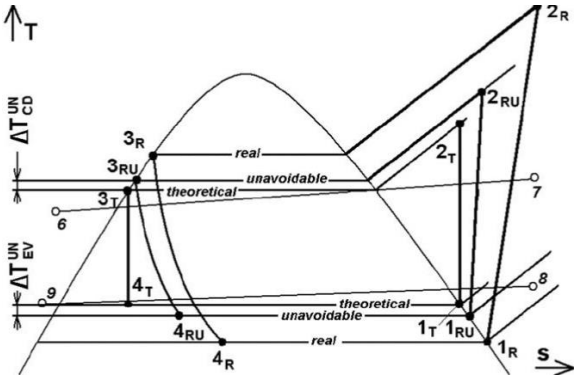

Figure 3. T-S graph of real and ideal cycles with unavoid. irreversibility [32].

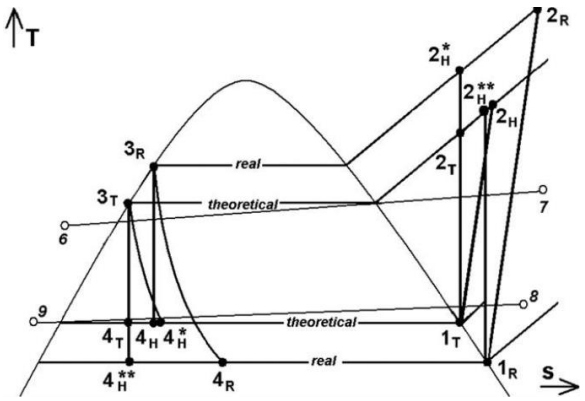

Figure 4. T-S graph of real cycle, ideal cycle and hybrid cycle for each component [32].

3. Validation

In order to confirm the validity of the simulation models, the information available in [32] has been used. The operating and design parameters in the whole cycle are assumed to be exactly the same as in this research, which are:

Table 2. Temperature (°C), heat (kW) and efficiency in a simple steam compression refrigeration cycle [32].

Parameter	T_1	T_7	T_3	$T_{theory-evap.}$	$T_{cond.RU}$	η_{comp}
Values	-25	30	40	-15	29.5	0.8
Parameter	T_8	T_6	T_9	$T_{theory-cond.}$	$T_{evap.-RU}$	Q_{cooler}
Values	-15	20	-15	28.65	-15.5	100

In this part, the results obtained from the analysis of exergy for the simple steam compression refrigeration cycle are presented. The results of applying the thermodynamic cycle method on the cycle shown in figure 2 are presented in table 3, and the results of [32] are presented in table 4. Various refrigerants have been used in this research. The goal of this research is not to examine these fluids, but the purpose is to determine impact of different materials characteristics on the advanced analysis of exergy results. For example, below only the tables related to R717 refrigerant is provided. According to tables 3 and 4, it is observed the agreement between the results of this research and results of [32], which proves the correctness of the method used in this research. These cycles include compressor (1), condenser (2), shut-off valve (3) and evaporator (4).

Table 3. Advanced analysis of exergy results on steam compression refrigeration cycle with R717 refrigerant for validation (present study).

												$\dot{E}^{UN}_{D,k}$		$\dot{E}^{AV}_{D,k}$	
component	$\dot{E}_{F,k}$	$\dot{E}_{P,k}$	$\dot{E}_{D,k}$	ϵ(%)	y_k	y^*_k	$\dot{E}^{th}_{D,k}$	$\dot{E}^{UN}_{D,k}$	$\dot{E}^{AV}_{D,k}$	$\dot{E}^{EN}_{D,k}$	$\dot{E}^{EX}_{D,k}$	$\dot{E}^{UN,EN}_{D,k}$	$\dot{E}^{UN,EX}_{D,k}$	$\dot{E}^{AV,EN}_{D,k}$	$\dot{E}^{AV,EX}_{D,k}$
1	43.12	37.36	5.763	86.6	13.4	19.6	0	0.860	4.902	3.845	1.917	0.829	0.032	3.017	1.886
2	15.08	2.38	12.69	15.8	29.4	43.3	2.888	3.427	9.265	8.049	4.644	3.238	0.188	4.81	4.455
3	22.83	18.69	4.148	81.8	9.6	14.1	1.504	1.82	2.328	1.734	2.414	1.734	0.085	0	2.328
4	18.14	11.42	6.719	62.9	15.6	22.9	2.141	2.361	4.358	6.719	0	2.361	0	4.358	0
Total	43.12	11.42	29.32	26.5	68.0	100	6.533	8.468	20.85	20.35	8.974	8.204	0.306	12.14	8.71
$\dot{m}^{real}_{R717} = 0.0962$ kg/s			$\dot{m}^{real}_{6-7} = 14.22\ kg/s$			$\dot{m}^{real}_{8-9} = 9.941\ kg/s$									

Table 4. Advanced analysis of exergy results on steam compression refrigeration cycle with R717 refrigerant for validation [32].

component	$\dot{E}_{F,k}$	$\dot{E}_{P,k}$	$\dot{E}_{D,k}$	$\epsilon(\%)$	y_k	y_k^*	$\dot{E}_{D,k}^{th}$	$\dot{E}_{D,k}^{UN}$	$\dot{E}_{D,k}^{AV}$	$\dot{E}_{D,k}^{EN}$	$\dot{E}_{D,k}^{EX}$	$\dot{E}_{D,k}^{UN}$		$\dot{E}_{D,k}^{AV}$	
												$\dot{E}_{D,k}^{UN,EN}$	$\dot{E}_{D,k}^{UN,EX}$	$\dot{E}_{D,k}^{AV,EN}$	$\dot{E}_{D,k}^{AV,EX}$
1	43.12	37.36	5.763	86.6	13.4	19.6	0	0.860	4.902	3.845	1.917	0.829	0.032	3.017	1.886
2	15.08	2.38	12.69	15.8	29.4	43.3	2.888	3.427	9.265	8.049	4.644	3.238	0.188	4.81	4.455
3	22.83	18.69	4.148	81.8	9.6	14.1	1.504	1.82	2.328	1.734	2.414	1.734	0.085	0	2.328
4	18.14	11.42	6.719	62.9	15.6	22.9	2.141	2.361	4.358	6.719	0	2.361	0	4.358	0
Total	43.12	11.42	29.32	26.5	68.0	100	6.533	8.468	20.85	20.35	8.974	8.204	0.306	12.14	8.71
$\dot{m}_{R717}^{real} = 0.0962$ kg/s			$\dot{m}_{6-7}^{real} = 14.22\ kg/s$			$\dot{m}_{8-9}^{real} = 9.941\ kg/s$									

With the thermodynamic cycle method in figure 2, the obtained results showed a good agreement between the results of [32] and our analysis in such a way that most of the results were the same or had little differences. Several differences between the results are due to the ideal consideration of exergy destruction in the expansion valve, which can be justified according to figure 3. According to this figure, it can be seen that there is an enthalpy difference in the 4T-3T process and by using that relation of exergy destruction, the value of ideal exergy loss of the expansion valve will not be zero. After that, the difference in results is in Unavoid. Exo. (40%)/Endo. (4%) exergy destruction.

4. Results and discussion

Separating exergy loss into unavoid./avoid. and endo./exo. parts has many benefit for detailed analyzes of power cycles. Combining the two exergy loss isolation approaches allows us to obtain the part of the exergy loss that rely on the inefficiency in a component that cannot be decreased due to the technological constraint. This means that it calculates the unavoid.endo. exergy loss. The endo. avoid. exergy loss is decreased through modifications in the target component. The exo. avoid. exergy loss illustrates the division of exergy loss that is decreased by optimizing of other components. It can also be concluded, reducing the amount of Endo. Avoid. exergy loss inside a component generally leads to the reduction of the exo.avoid. exergy loss in alternative components.

In steam cycle simulation, simplification is needed. The assumptions considered are as follows:

1. All of the process in in CSP plant is assumed to be stable.
2. The expansion action in the valve is assumed to be enthalpy constant.
3. The output power of the power plant is 10MW and a constant value is assumed.
4. The outlet of the aerator is saturated liquid.
5. In the heat exchange between the steam part and the solar part, we consider ΔT at the exit from the economizer and superheat. Its values are equal to: $\Delta T_{ECO} = 15.7$ and $\Delta T_{SH} = 15.56$.
6. The outlet of the condenser is in saturated liquid state.
7. The isentropic efficiency of turbines, pumps, evaporator, heat exchanger, mechanical efficiency of turbine, mechanical and electrical efficiency of turbine engine and efficiency of auxiliary equipment are given in table 5:

Table 5. Assumptions of components efficiency in steam part of the solar steam power plant [33].

Efficiency (%)	HPT	LPT	Pumps	Boiler	HE	Mechanical turbine	Mech. and Elec. eff. of extracted steam from turbine	Auxiliary equipment
values	85	90	80	96	96	90	95	97

In solving thermodynamic equations, it is necessary to consider a number of cycle parameters including temperature and pressure of some known points. These parameters are listed in table 6.

Table 6. Temperature and pressure assumptions of the components of the steam part of the CSP [33].

	Pressure (bar)					Temperature (˚C)					
Parameter	Boiler	Condenser	Cogeneration extraction	Regeneration extraction	Reheater	Boiler	Reheater	H.E output	H.E Input	Cond. Input	Cond. Output
Values	95	0.05	5	10	15	500	420	100	70	25	30

Figure 5 shows the schematic of the power plant and figure 6 shows the actual cycle T-s diagram of the steam part of theCSP plant. The boiler exchanges heat with the solar unit in three stages, which can be clearly seen in the figure. The steam part consists of 3 pumps, expansion valve, boiler (which includes economizer, evaporator and superheater), LPT, HPT, HE, condenser, and deaerator.

In the boiler (including economizer, evaporator, and superheater), water is heated and its energy is supplied to drive the HPT. In this way, the water

in the economizer becomes a saturated liquid. Then in the evaporator, the saturated liquid absorbs heat and becomes vapor saturated at the same temperature. Finally, it reaches the superheated state in superheater.

Part of the extracted steam from the high pressure turbine is deaerated after passing through the expansion valve and then pumped to the boiler, but the main part of it goes to the low pressure turbine after reheating in the Re-heater. The low pressure turbine has two extracted steam. One of them is cooled by the condenser and the other is cooled by the heat exchanger and then pumped to the aerator. An aerator is a widely used device for removing oxygen and other dissolved gases from water. The aerator output is also pumped to the boiler.

After coding related to the cycle and solving the relevant thermodynamic equations, the working conditions and thermodynamic characteristics of different points of the steam part of solar steam power plant under the assumed conditions is shown in table 7. Also some characteristics of the points of the solar part of the cycle that are in contact with the steam part are given in tables 8 and 9.

In table 10, the results obtained from the simulation of the steam part are compared with reference [33]. According to the agreement of the results of the present work with the results of [33], it is possible to prove the correctness of the method and relationships. The biggest error is in η_{plant}, which according to the plant efficiency relation can be seen that the result of the present work is correct.

Table 11 demonstrates the exergy loss in all components. In figure 7, the circular diagram shows the proportion of exergy dissipation of each component to the total exergy dissipation of the cycle. As can be seen, maximum and minimum exergy loss are occurred in the evaporator and pumps, respectively.

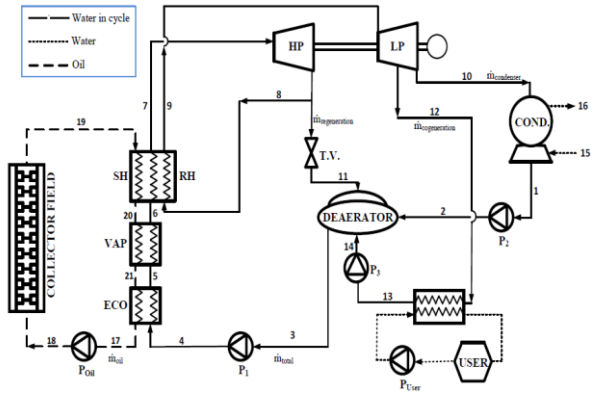

Figure 5. Schematic of CSP plant cycle.

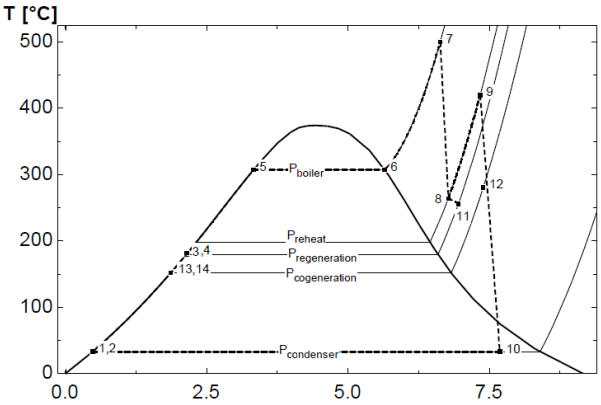

Figure 6. T-S graph of the actual steam part of the solar steam power plant.

Table 7. Characteristics of different nodes of the actual cycle of the solar part.

Nodes	T (˚C)	S (KJ/kg-˚K)	P (bar)	H (KJ/kg)	$\dot{m}(\frac{kg}{s})$	Ex(MJ/kg)	X
1	32.88	0.4761	0.05	137.7	6.651	0.0003317	0
2	32.97	0.4769	10	139	6.651	0.001338	-
3	179.9	2.139	10	762.8	10.21	0.1297	0
4	181.6	2.144	95	774.7	10.21	0.1401	-
5	307.3	3.323	95	1385	10.21	0.3993	0
6	307.3	5.645	95	2733	10.21	1.055	1
7	500	6.627	95	3380	10.21	1.409	-
8	264.2	6.771	15	2956	8.229	0.9417	-
9	420	7.332	15	3299	8.229	1.118	-
10	32.88	7.68	0.05	2342	6.651	0.05711	0.9099
11	256.3	6.95	10	2956	1.98	0.8882	-
12	280.7	7.388	5	3024	1.578	0.8256	-
13	151.8	1.861	5	640.3	1.578	0.09004	0
14	151.9	1.861	10	641	1.578	0.09063	-
15	25	0.3669	1.013	104.8	701	0	-
16	30	0.4365	1.013	125.8	701	0.0001734	-

Table 8. Characteristics of the points of the solar part in contact with the steam part of the real

Points	17	19	20	21
T (˚C)	264.1	515.5	453.1	323
$\dot{m}(kg/s)$	37.28	37.28	37.28	37.28

Table 9. Characteristics of different components in the solar part.

Component	C_f	ΔH	ΔS	$\Delta\dot{E}$
Economizer	2.913	171.6	0.3031	0.08124
Evaporator	3.264	424.6	0.6442	0.2325
Superheater and Reheater	3.62	225.9	0.2984	0.1369

Table 10. Simulation results of steam part in CSP.

Parameter	Present work	Previous study [33]	Error (%)
η_{cycle}	0.3589	0.3588	0.02
η_{plant}	0.3263	0.4442	26.54
$\dot{m}_{cogeneration}\ [kg/s]$	1.578	1.58	0.12
$\dot{m}_{total}\ [kg/s]$	10.21	10.21	0
$\dot{m}_{regeneration}\ [kg/s]$	1.98	1.98	0
Q [MW]	30.65	30.66	0.03
$W_{turbine}[MW]$	11	11	0

Table 11. Exergy destruction of steam cycle components of solar steam power plant.

Component	Pump2	Deaerator	Pump1	Economizer	Evaporator	Superheater & Reheater
$\dot{E}_D$	0.00162	0.5861	0.016	0.3824	1.976	0.04351
Component	High pressure turbine	Expansion valve	Low pressure turbine	Condenser	Pump3	Heat exchanger
$\dot{E}_D$	0.4374	0.1058	0.7152	0.2561	0.0001513	0.5294

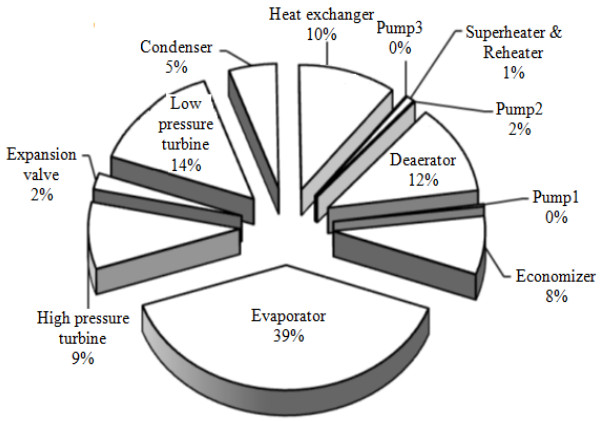

Figure 7. Real exergy destruction of components of steam part under assumed conditions.

In figure 8, the graph of the energy and exergy efficiency changes for the condenser pressure changes at three boiler temperatures of 450 ºC, 500 ºC, and 550 ºC at a boiler pressure of 95 bar; and in figure 9, the diagram of the energy and exergy efficiency changes for the condenser pressure changes at three pressures of 80 bar, 95 bar, and 110 bar at the boiler temperature of 500 ºC is given.

As can be seen from these graphs, when condenser pressure is raised, the energy and exergy efficiency of the entire cycle is reduced. Also increasing the temperature and pressure of the boiler increases the energy and exergy efficiency of the entire cycle.

In the description of the mentioned diagrams, it can be said that from the T-s diagram of the examined cycle (Figure 6), it can be seen that the increase in pressure causes the decrease in enthalpy changes in it. Considering the constant heat flow rate that the condenser loses, then the mass flow rate passing through it must be increased; As a result, this causes an increase in the rest of the mass flow rate. According to the relationships of the energy equations for the whole cycle, increasing the mass flow rate increases the total heat flow rate, the total fuel input exergy flow rate, and the exergy destruction flow rate. Since the power plant and cycle are assumed to be constant, as a result, the efficiency of the first and second law decreases. Also with rising the boiler temperature and pressure, efficiencies are enhanced. Because the cycle operates in more critical conditions.

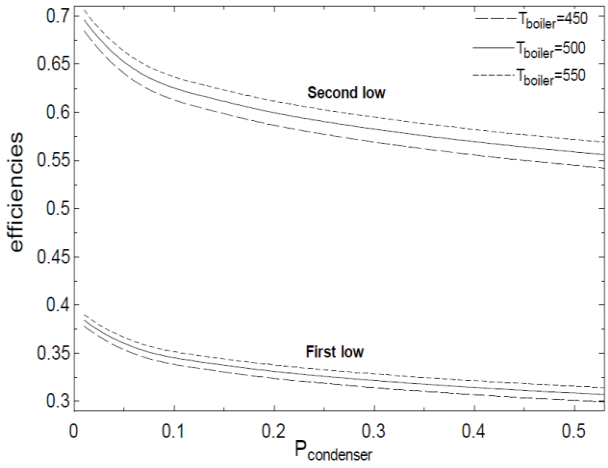

Figure 8. Energy and exergy efficiency variations versus condenser pressure changes at different boiler temperatures and at P_boiler = 95 bar.

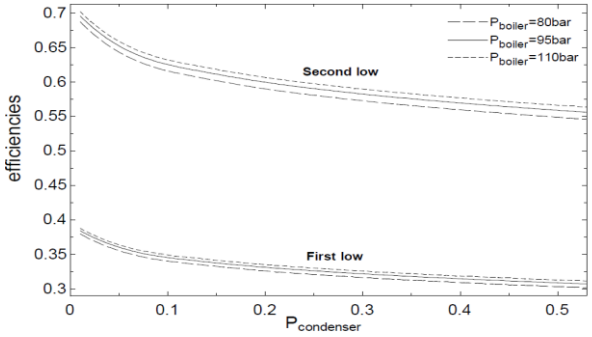

Figure 9. Energy and exergy efficiency Variations versus the condenser pressure changes at different boiler pressures and at T_boiler = 500 ºC.

It is critical to examine the exergy dissipation changes of entire cycle against different parameters of the cycle, such as boiler temperature and pressure, reheating temperature and pressure, turbine pressure, mass flow rate, etc. Examining all of the above changes for all components of the cycle is not the goal of this research, but due to the importance of the matter, here only the examination of the changes of the exergy dissipation of the entire cycle with the changes of P_cogeneration, P_regeneration, and P_condenser pressures is shown in figure 10.

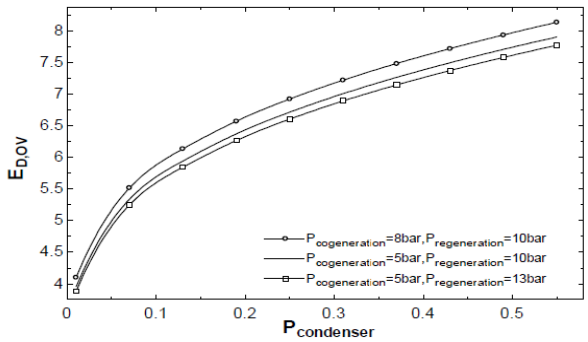

Figure 10. Changes of exergy loss of the entire cycle versus the changes of P_cogeneration, P_regeneration, and P_condenser pressures.

From this figure, it can be seen that the pressure of the co-production as well as the condenser pressure is caused a growth in the total system exergy loss. However, the pressure of regeneration works in the opposite way, which can be attributed to the negative effect of excessive regeneration.

In order to form an ideal cycle, it is necessary for all cycle components to work ideally with zero or minimal exergy destruction, for this the turbine and pumps must work with 100% efficiency and all heat exchangers act with zero temperature difference or close to zero. Tables 12, 13, and 14 show the thermodynamic characteristics of all ideal cycle points.

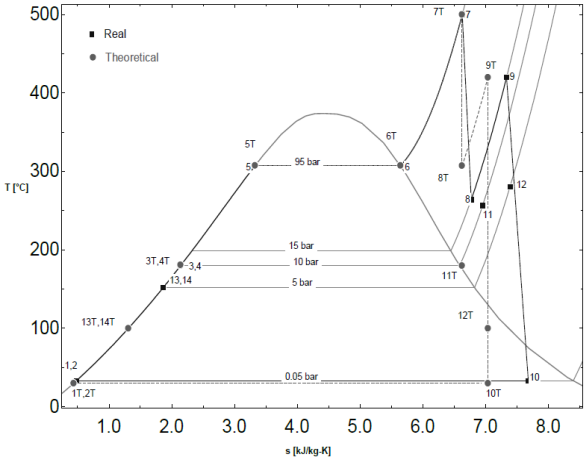

Figure 11. T-S chart of the ideal and actual cycle of the steam part of the solar steam power plant (dashed line: ideal cycle, continuous line: actual cycle).

Table 12. Characteristics of the points of the solar part in contact with the steam part of the ideal cycle under the assumed conditions.

Point	17	19	20	21
$T\ [^{\circ}C]$	248.64	500.04	437.64	307.54
$\dot{m}\ [kg/s]$	29.84	29.84	29.84	29.84

Table 13. Characteristics of solar points in contact with the steam part of the ideal cycle under assumed conditions.

Component	C_f	ΔH	ΔS	$\Delta \dot{E}$
Economizer	2.856	168.2	0.3055	0.07715
Evaporator	3.206	417.1	0.6482	0.2239
Superheater & Reheater	3.563	222.3	0.2998	0.1329

Table 15 shows the exergy dissipation when the cycle is operating ideally and figure 12 shows the pie chart of the exergy dissipation in the CSP under ideal conditions.

Table 14. Characteristics of different points of the ideal cycle of the steam part of the solar steam power plant.

point	$T\ [^{\circ}C]$	S [kj/kg-˚C]	P [bar]	H [kjkg]	$\dot{m}$ [kg/s]	Ex [Mj/kg]	X
1	30	0.4365	0.04246	125.7	4.961	0.00007608	0
2	30.02	0.4365	10	126.7	4.961	0.001076	-
3	179.9	2.139	10	762.8	8.57	0.1297	0
4	181.1	2.139	10	762.8	8.57	0.1297	0
5	307.5	3.325	95.34	1387	8.57	0.4	0
6	307.5	5.643	95.34	2733	8.57	1.055	1
7	500	6.625	95.34	3380	8.57	1.409	-
8	307.7	6.625	27.24	3019	6.721	1.409	-
9	420	7.037	27.24	3281	6.721	1.187	-
10	30	7.037	0.04246	2127	4.961	0.03308	0.8235
11	179.9	6.625	10	2795	1.849	0.8248	-
12	99.97	7.037	1.013	2557	1.76	0.4636	0.9474
13	100	1.037	1.013	419.1	1.76	0.03397	0
14	100.1	1.037	10	420	1.76	0.03491	-

Table 15. Exergy destruction of the components of the ideal cycle of the steam power plant in the assumed conditions.

Component	Pump2	Deaerator	Pump1	Economizer	Evaporator	Superheater & Reheater
$\dot{E}_D$	0	0.4805	0	0.06767	1.069	0.000136
Component	High pressure turbine	Expansion valve	Low pressure turbine	Condenser	Pump3	Heat exchanger
$\dot{E}_D$	0	0.4137	0	0.08141	0	0.1244

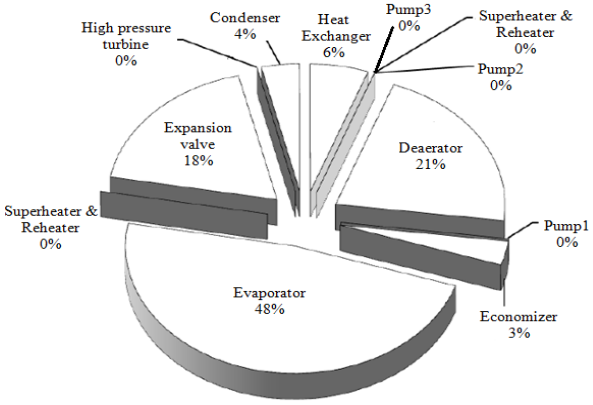

Figure 12. Exergy loss of steam part components in an ideal power plant under assumed conditions.

As it is clear from table 15, the exergy loss of each components of the ideal cycle is either zero or at least; what is clear is the exergy dissipation reduction of the all components of the ideal cycle compared to the real cycle.

Table 16 presents the results of conventional exergy analysis and simulation of the ideal cycle for all components; in this table, all exergy values are in megawatts. The only exception is the expansion valve, which in the ideal case has more exergy destruction than in the actual case. Of course, this increase is insignificant and can be ignored compared to the amount of decrease that occurs in the exergy destruction of the whole system.

In the next parts, the results of separating the exergy dissipation of each component into Endo., Exo., Avoid., and Unavoid. components are discussed.

Table 16. Conventional results for each of the steam cycle components of the solar steam power plant.

Component	$\dot{E}_F$	$\dot{E}_P$	$\dot{E}_D$	ϵ	y	y^*	$\dot{E}_{D,Th}$
Pump2	0.0083	0.0067	0.0016	0.8052	0.0001	0.00032	0
Deaerator	1.91	1.3240	0.5861	0.6932	0.03489	0.11606	0.4805
Pump1	0.122	0.1061	0.016	0.8688	0.0095	0.00317	0
Economizer	3.029	2.6460	0.3824	0.8737	0.02276	0.07572	0.0677
Evaporator	8.669	6.693	1.976	0.772	0.11762	0.39129	1.069
High pressure turbine	4.77	4.333	0.4373	0.9083	0.02603	0.08659	0
Expansion valve	0.9624	0.9086	0.1058	0.9441	0.0063	0.02095	0.4137
Low pressure turbine	7.514	6.798	0.7152	0.9048	0.04257	0.14162	0
Condenser	0.3777	0.1216	0.2561	0.322	0.01524	0.05071	0.0814
Heat Exchanger	1.161	0.6316	0.5294	0.5440	0.03151	0.10483	0.1244
Pump3	0.0011	0.0009	0.0002	0.8597	0.00001	0.00003	0
Superheater & Reheater	5.105	5.062	0.0435	0.9915	0.00259	0.00862	0.0001
Total	16.8	11.63	5.0496	0.6547	0.3006	1	2.2368

Endo. and exo. components:

In this section, the results of dividing the exergy loss of each cycle component into exo. and endo. parts are presented. Figures 13 and 14 show a bar chart related to this division for the components of the cycle and the overall cycle, respectively.

According to the results obtained in figures 13 and 14, it can be said that the contribution of the Endo. factor is higher in all components. This indicates that the component itself inefficiency has a greater influence on the exergy loss occurring in the component and the effect of external factors such as the inefficiency of other components is less than the impact of the component itself inefficiency. In the case of low pressure turbine, throttle valve, third pump, superheater and reheater, the value of the Endo. factor is greater than the exergy destruction of the desired component and the Exo. factor is negative. This means that the improvement in other components causes an increase in exergy dissipation in these components and to improve them the exergy dissipation of other components of the cycle must increase, which will increase the exergy loss of the cycle. As it is clear from the above discussion, classifying exergy loss into exo. and endo. parts increases the researchers' understanding of the meaning of exergy loss and displays how much irreversibility can be eliminated to enhance the cycle.

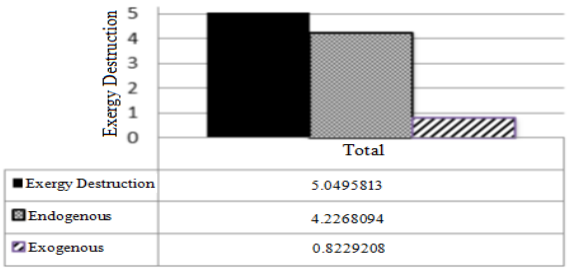

Figure 13. Division of exergy loss of the steam cycle into endo. and exo. components.

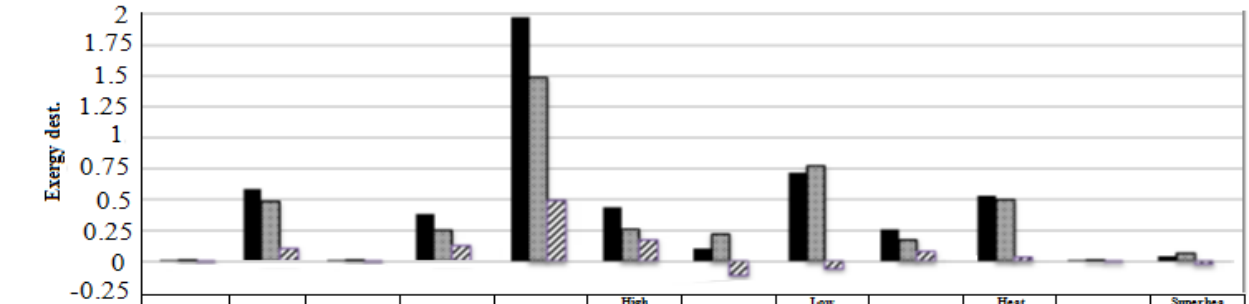

	Pump2	Deaerator	Pump1	Economizer	Evaporator	High pressure turbine	Expansion valve	Low pressure turbine	Condenser	Heat exchanger	Pump3	Superheater & Reheater
Exergy dest.	0.00162	0.5861	0.016	0.3824	1.976	0.4373	0.1058	0.7152	0.2561	0.5294	0.00015	0.04551
Endogenous	0.00122	0.4805	0.01351	0.2525	1.484	0.2607	0.2208	0.7721	0.1763	0.4968	0.00033	0.06805
Exogenous	0.0004	0.1056	0.00249	0.1297	0.4924	0.1766	-0.115	-0.05687	0.0798	0.03252	-0.0002	-0.02454

Figure 14. Exergy loss division for each component into exo. and endo. components.

Avoid. and Unavoid. components:

Avoid. and Unavoid. components of exergy loss of each component actually show the capability of a component to improve efficiency by reducing irreversibility. In other words, these values show how far the advancement of industry technology allows researchers to reduce the amount of irreversibility in a component. Figures 15 and 16 show the bar chart of exergy loss divided into unavoid. and avoid. factors for the overall cycle and cycle components, respectively.

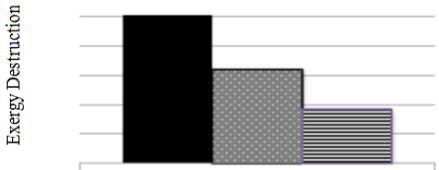

	Total
Exergy Destruction	5.0495813
Endogenous	3.19885486
Exogenous	1.85072589

Figure 15. Division of exergy loss of the steam part into avoid. and unavoid. components.

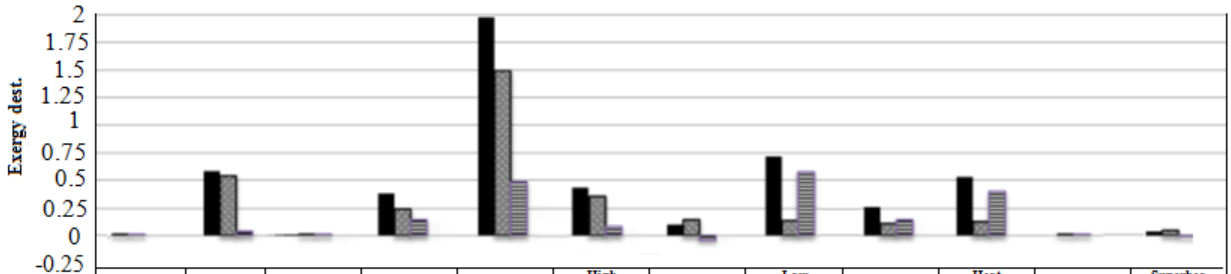

	Pump2	Deaerator	Pump1	Economizer	Evaporator	High pressure turbine	Expansion valve	Low pressure turbine	Condenser	Heat exchanger	Pump3	Superheater & Reheater
Exergy dest.	0.00162	0.5861	0.016	0.3824	1.976	0.4373	0.1058	0.7152	0.2561	0.5294	0.00015	0.04351
Avoidable	0.00028	0.5426	0.00297	0.2404	1.49	0.358	0.1422	0.1362	0.112	0.1284	6.6E-05	0.04574
Unavoidable	0.00234	0.04356	0.01304	0.142	0.4858	0.07929	-0.0364	0.5791	0.1441	0.401	8.5E-05	-0.0022

Figure 16. Exergy loss division of each cycle component into Avoid. and Unavoid. Components.

According to the results shown in figures 15 and 16, in pump 1, pump 2, economizer, low pressure turbine, condenser and heat exchanger, the contribution of the Avoid. factor in exergy destruction is higher and a major part of exergy destruction can be eliminated. In the throttle valve, aerator, evaporator, high-pressure turbine, pump 3, superheater and re-heater is the contribution of the Unavoid. factor, which means that compared to other components, they have less potential to reduce irreversibility.

Endo. Unavoid., Exo. Unavoid., Endo. Unavoid., and Exo. Unavoid. components

In this part, the Endo. or Exo. exergy loss of the cycle components is investigated. By calculating each of these components, it is possible to determine the contribution of industry progress to the reduction of exergy loss of each component through the component itself and other components. In fact, the endo. avoid. part represents a part of the exergy loss of the component that is able to avoided by enhancing the structure of the component itself, and the exo. avoid. part represents a part of component exergy destruction, which is avoided by enhancing the structure of other components. The unavoid. endo. and exo. parts are the portion of the exergy loss of the component which cannot be reduced even by

refining the structure of the component and other components.

This division is done in figure 17 for the whole cycle in figures 18 to 29 for each cycle component. Also the advanced analysis results are given in table 17. In this form and table, all the values obtained for exergy destruction will be in megawatts.

Table 17. Results of separation of exergy destruction with advanced exergy method.

						Unavoid.		Avoid.	
Component	Exergy Dest.	Exo.	Endo.	Avoid.	Unavoid.	Endo. Unavoid.	Exo. Unavoid.	Endo. Avoid.	Exo. Avoid.
Pump2	0.0016	0.0004	0.0012	0.0013	0.0003	0.000257	0.000026	0.000963	0.000374
Deaerator	0.5861	0.1056	0.4805	0.0436	0.5426	0.480500	0.062040	0	0.0430560
Pump1	0.0160	0.0025	0.00135	0.0130	0.0030	0.002842	0.000124	0.010670	0.002365
Economizer	0.3824	0.1297	0.2525	0.1420	0.2404	0.198600	0.041860	0.054190	0.087810
Evaporator	1.9760	0.4924	1.4840	0.4858	1.4900	1.3400	0.1501	0.1434	0.3423
High pressure turbine	0.4373	0.1766	0.2607	0.0793	0.3580	0.0642	0.2938	0.1964	-0.1172
Expansion valve	0.1058	-0.1150	0.2208	-0.0364	0.1422	0.2208	-0.0786	0	-0.0364
Low pressure turbine	0.4373	0.1766	0.2607	0.0793	0.3580	0.06424	0.2938	0.1964	-0.1172
Condenser	0.2561	0.0798	0.1763	0.1441	0.1120	0.09781	0.014170	0.07845	0.06564
Heat Exchanger	0.5294	0.0325	0.4968	0.4010	0.1284	0.1284	0	0.3684	0.0325
Pump3	0.0002	-0.0001	0.0003	0.0001	0.0001	0.00007	-0.000003	0.0007	-0.00018
Superheater & Reheater	0.0435	-0.0245	0.0681	-0.0022	0.0457	0.05791	0.01217	0.01013	0.01237
Total	5.0496	0.8229	4.2268	1.8507	3.1989	2.7271	0.47174	1.4993	0.35117

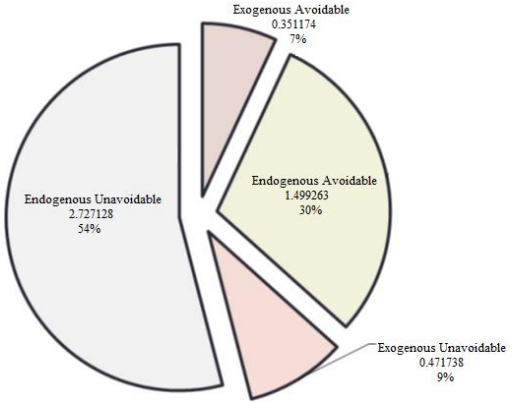

Figure 17. Exergy loss division of the steam part of the CSP.

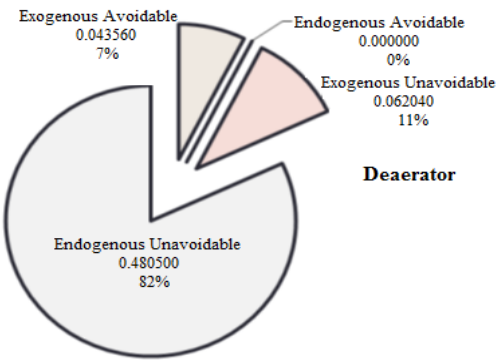

Figure 18. Deaerator exergy destruction division.

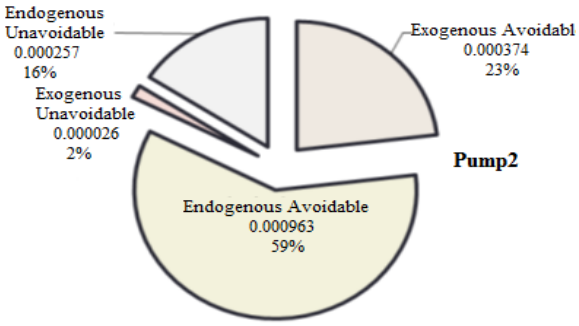

Figure 19. Division of pump 2 exergy destruction.

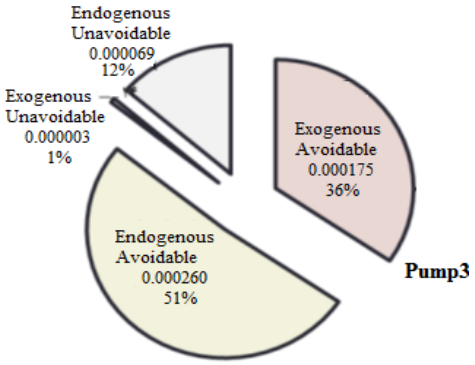

Figure 20. Division of pump 3 exergy destruction.

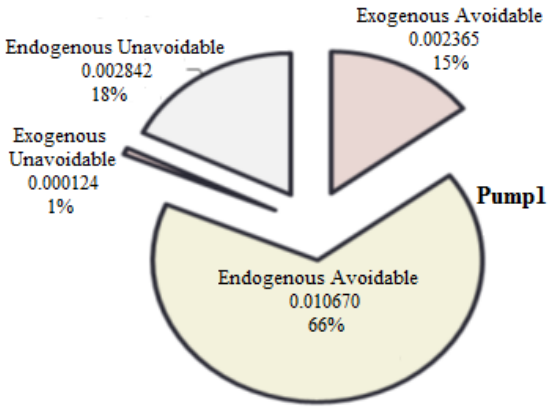

Figure 21. Division of pump 1 exergy destruction.

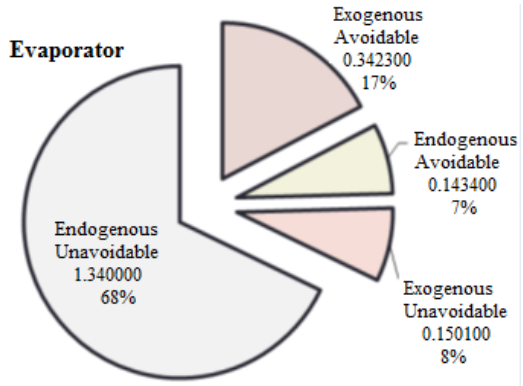

Figure 22. Evaporator exergy destruction division.

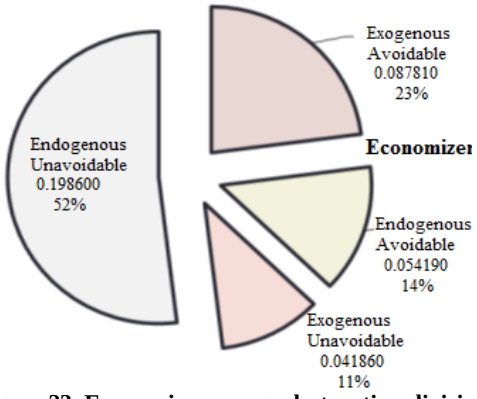

Figure 23. Economizer exergy destruction division.

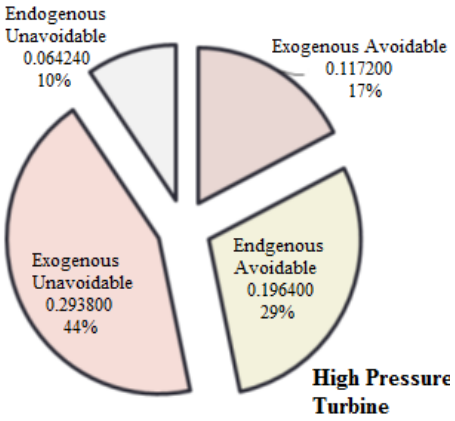

Figure 24. High pressure turbine exergy destruction division.

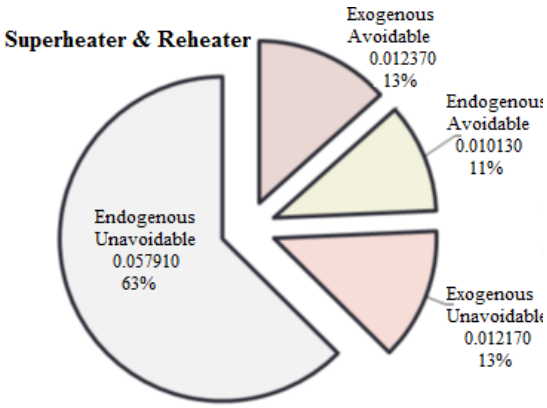

Figure 25. Superheater & Reheater exergy destruction division.

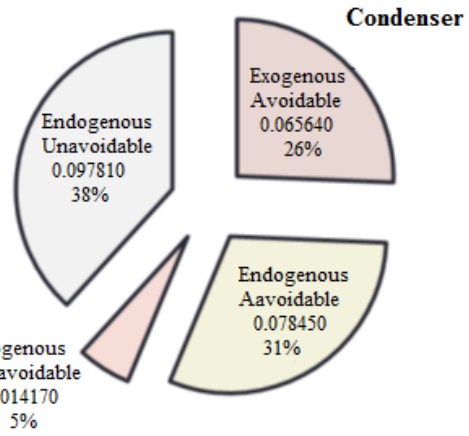

Figure 26. Condenser exergy destruction division.

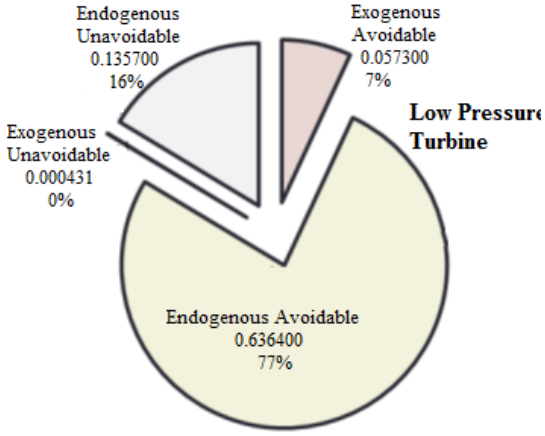

Figure 27. Low pressure turbine exergy destruction division.

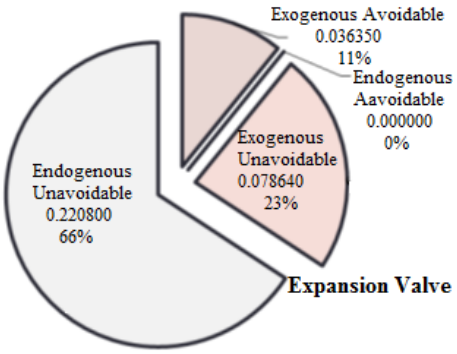

Figure 28. Expansion valve exergy destruction division.

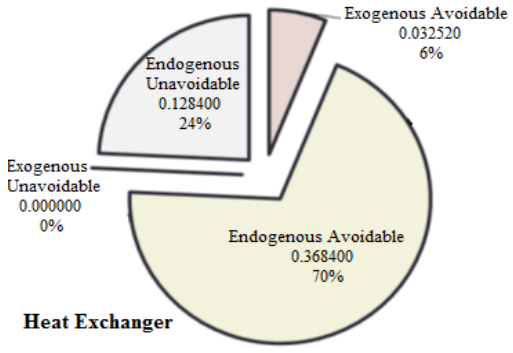

Figure 29. Heat exchanger exergy destruction division.

In accordance with analysis performed in this section, it can be said that in the performance of

the steam part of theCSP plant with the presented structure, the most exergy destruction is related to the evaporator, low pressure turbine, aerator, heat exchanger and high pressure turbine respectively, which is obtained from the conventional exergy analysis. To improve the cycle, one should start from the low pressure turbine because it has the highest amount of Avoid. and Endo. factors. After that, there are heat exchanger, high pressure turbine and evaporator. Also, the evaporator has the highest exo. avoid. value. This means that the evaporator has the most effectiveness from the inefficiency of other components and the other components enhancement has the most positive influence on it. The Avoid. inefficiency of pumps, turbines, heat exchangers, condensers, expansion valves, superheaters, and reheaters has a greater effect on the destruction exergy of component while in the evaporator, economizer and air conditioner, the other components enhancement has a greater influence on decreasing the exergy loss than the component itself refinement. Because in these components, the exo. avoid. factor is greater than the endo. avoid. factor. In the examination of the unevoidable exergy destruction of the components, it has been determined that maximum Unavoid. exergy loss is occurred in the evaporator and the major contribution of this irreversibility is associated with component itself inefficiency. The deaerator is also in the next step with such conditions.

5. Conclusion

Advanced analysis of exergy is a useful tool for cycle thermodynamic analysis. Dividing exergy loss in a cycle into exo., endo., avoid., and unavoid. parts can be very useful for thermoeconomic analysis and for reducing irreversibilities and improving cycle performance. This analysis shows the quantity of exergy dissipation in each component, finding the cause of this exergy destruction, the ability and potential to improve each component and the ability to decrease the exergy dissipation of the component.
In this study, the influence of the components on each other and the improvement potential of each of them have been investigated, and the following results have been obtained:

1. Total exergy loss of the cycle is 5.0496 MW.
2. Pumps have the least exergy destruction. Therefore, they are the most efficient components of the CSP.
3. Superheater and reheater have the highest exergy efficiency.
4. The maximum exergy loss is occurred in the evaporator, LPT, aerator, HE and HPT, respectively, which is obtained from conventional analysis. Its value in the evaporator is 1.976, of which 68% (1.34 MW) is as Unavoid. Endo. type.
5. Exergy dissipation of components in this cycle is mostly due to the inefficiency of the component itself and they are less affected by other components.
6. In pump 1, pump 2, economizer, low pressure turbine, condenser and heat exchanger, the contribution of the Avoid. factor in exergy loss is higher and a major portion of exergy loss can be eliminated. In expansion valves, air blowers, evaporators, high pressure turbines, pump 3, superheaters, and reheaters, the contribution of the Unavoid. factor is higher, which means that compared to other components, they have less potential to reduce irreversibility.
7. Results show that the endo. exergy loss inefficiency of turbines, pumps, heat exchangers, condensers, Expansion valves, superheaters and reheaters have more share of total exergy loss of component.
8. In the evaporator, economizer and deaerator, optimizing other components has a greater effect on reducing component exergy loss.
9. Due to having the largest amount of Endo. Avoid. factor, to improve the cycle, one should start from the low pressure turbine first. The LPT has the maximum Endo. Avoid. amount of exergy destruction (0.6364 MW) and in the next steps are the HE, HPT and evaporator.
10. Evaporator is significantly influenced by the other components performance and enhancement of other components has the most positive effect on it, because it has the largest amount of Exo. Avoid.

6. Nomenclature

Avoid.	Avoidable
Unavoid.	Unavoidable
Endo.	Endogenous
Exo.	Exogenous
CSP	Concentrated solar power
IGCC	Integrated gasification combined cycle
PEMFC	Proton exchange membrane fuel cell
HE	Heat exchanger
HPT	High pressure turbine
LPT	Low pressure turbine
HE	Heat exchanger
Eff.	Efficiency
Mech.	Mechanical
Elec.	Electrical

CCPP	Combined cycle power plant
ORC	Organic Rankine cycle

7. References

[1] A. Mehrpanahi, S. Nikbakht Naserabad, and G. Ahmadi. Multi-objective linear regression based optimization of full repowering a single pressure steam power plant. Energy. 179 (2019) 1017-1035.

[2] M.A. Vakilabadi, M. Bidi, A. Najafi, and M.H. Ahmadi. Exergy analysis of a hybrid solar-fossil fuel power plant. Energy Science & Engineering. 7 (2019) 146-61.

[3] M.A. Vakilabadi, M. Bidi, and A. Najafi. Energy, Exergy analysis and optimization of solar thermal power plant with adding heat and water recovery system. Energy conversion and management. 171 (2018) 1639-50.

[4] M. Akbari Vakilabadi, M. Bidi, A. Najafi, and M.H. Ahmadi. Energy, exergy analysis and performance evaluation of a vacuum evaporator for solar thermal power plant zero liquid discharge systems. Journal of Thermal Analysis and Calorimetry. 139 (2020) 1275-90.

[5] A. Saedi, A. Jahangiri, M. Ameri, and F. Asadi. Feasibility study and 3E analysis of blowdown heat recovery in a combined cycle power plant for utilization in Organic Rankine Cycle and greenhouse heating. Energy. 260 (2022) 125065.

[6] M. Akbari Vakilabadi, A. Binesh, and M. Monfared. Hydrodynamic Behavior of Biomass Micro-Particles in Counter-Flow Combustion of Dust Clouds. Renewable Energy Research and Applications. 4 (2023) 55-66.

[7] M. Bidabadi, M.A. Vakilabadi, A. Esmaeilnejad. Strain rate effect on microorganic dust flame in a premixed counterflow. Heat Transfer Research. 46 (2015.

[8] T. Koroglu, O.S. Sogut. Conventional and advanced exergy analyses of a marine steam power plant. Energy. 163 (2018) 392-403.

[9] M. Elhelw and K.S. Al Dahma. Utilizing exergy analysis in studying the performance of steam power plant at two different operation mode. Applied Thermal Engineering. 150 (2019) 28.93-5

[10] L. Cai, Y. Fu, Z. Cheng, Y. Xiang, and Y. Guan. Advanced exergy and exergoeconomic analyses to evaluate the economy of LNG oxy-fuel combined cycle power plant. Journal of Environmental Chemical Engineering. 10 (2022) 108387.

[11] Y. Cao, F. Rostamian, M. Ebadollahi, M. Bezaatpour, and H. Ghaebi. Advanced exergy assessment of a solar absorption power cycle. Renewable Energy. 183 (2022) 561-74.

[12] L. Anetor, E.E. Osakue, and C. Odetunde. Classical and advanced exergy-based analysis of a 750 MW steam power plant. Australian Journal of Mechanical Engineering. 20 (2022) 448-68.

[13] O.R. Altarawneh, A.A. Alsarayreh, M. Ala'a, M.J. Al-Kheetan, and S.S. Alrwashdeh. Energy and exergy analyses for a combined cycle power plant in Jordan. Case Studies in Thermal Engineering. 31 (2022) 101852.

[14] A. Basem, M. Moawed, M.H. Abbood, and W.M. El-Maghlany. The energy and exergy analysis of a combined parabolic solar dish–steam power plant. Renewable Energy Focus. 41 (2022) 55-68.

[15] Y. Dai, J. Wang, and L. Gao. Exergy analysis, parametric analysis and optimization for a novel combined power and ejector refrigeration cycle. applied thermal engineering. 29 (2009) 1983-90.

[16] H. Montazerinejad, E. Fakhimi, S. Ghandehariun, and P. Ahmadi. Advanced exergy analysis of a PEM fuel cell with hydrogen energy storage integrated with organic Rankine cycle for electricity generation. Sustainable Energy Technologies and Assessments. 51 (2022) 101885.

[17] M. Song, Y. Zhuang, L. Zhang, C. Wang, J. Du, and S. Shen. Advanced exergy analysis for the solid oxide fuel cell system combined with a kinetic-based modeling pre-reformer. Energy Conversion and Management. 245 (2021) 114560.

[18] Y. Şöhret, E. Açıkkalp, A. Hepbasli, and T.H. Karakoc. Advanced exergy analysis of an aircraft gas turbine engine: splitting exergy destructions into parts. Energy. 90 (2015) 1219-28.

[19] J. Sheng, M. Voldsund, and I.S. Ertesvåg. Advanced exergy analysis of the oil and gas processing plant on an offshore platform: A thermodynamic cycle approach. Energy Reports. 9 (2023) 820-32.

[20] Y. Tian, T. Zhang, N. Xie, Z. Dong, Z. Yu, M. Lyu *et al*. Conventional and advanced exergy analysis of large-scale adiabatic compressed air energy storage system. Journal of Energy Storage. 57 (2023) 106165.

[21] A. Ustaoglu, H. Torlaklı, A. Ergün, E. Erdoğmuş, and M.E. Akay. Advanced exergy analysis of an integrated solid waste fueled cogeneration system based on organic Rankine Cycle for different working fluids. Energy Conversion and Management. 270 (2022) 116294.

[22] X. Zhong, T. Chen, X. Sun, J. Song, and J. Zeng. Conventional and advanced exergy analysis of a novel wind-to-heat system. Energy. 261 (2022) 125267.

[23] M. Ezzat and I. Dincer. Energy and exergy analyses of a novel ammonia combined power plant operating with gas turbine and solid oxide fuel cell systems. Energy. 194 (2020) 116750.

[24] H. Yan, M. Liu, D. Chong, C. Wang, and J. Yan. Dynamic performance and control strategy comparison of a solar-aided coal-fired power plant based on energy and exergy analyses. Energy. 236 (2021) 121515.

[25] J. Zueco, D. López-Asensio, F. Fernández, and L.M. López-González. Exergy analysis of a steam-turbine power plant using thermocombustion. Applied Thermal Engineering. 180 (2020) 115812.

[26] A. Kumar, K. Nikam, and A.K. Behura. An exergy analysis of a 250 MW thermal power plant. Renewable Energy Research and Applications. 1 (2020) 197-204.

[27] S. Zhang, M. Liu, Y. Zhao, K. Zhang, J. Liu, and J. Yan. Thermodynamic analysis on a novel bypass steam recovery system for parabolic trough concentrated solar power plants during start-up processes. Renewable Energy. 198 (2022) 973-83.

[28] S. Zhang, M. Liu, Y. Zhao, J. Liu, and J. Yan. Energy and exergy analyses of a parabolic trough concentrated solar power plant using molten salt during the start-up process. Energy. 254 (2022) 124.480

[29] Y. Zhao, M. Liu, J. Song, C. Wang, J. Yan, and C.N. Markides. Advanced exergy analysis of a Joule-Brayton pumped thermal electricity storage system with liquid-phase storage. Energy Conversion and Management. 231 (2021) 113867.

[30] K. Maghsoudi Mehrabani, A. Mehrpanahi, V. Rouhani, and S. Nikbakht Naserabad. Study of the effect of using duct burner on the functional parameters of the two repowered cycles through exergy analysis. Thermal Science. 2 (6 Part B) (2017) 3011-3023.

[31] K. Maghsoudi Mehrabani, A. Mehrpanahi, V. Rouhani, and S. Nikbakht Naserabad. Using two types of heat recovery steam generator for full repowering a steam power plant and its analysis by exergy method. Indian Journal of Scientific Research. 1(2) (2014), 183-198.

[32] T. Morosuk and G. Tsatsaronis. Advanced exergy analysis for chemically reacting systems–application to a simple open gas-turbine system. International Journal of Thermodynamics. 12 (2009) 105-11.

[33] A. Kolios, S. Paganini, and S. Proia. Development of thermodynamic cycles for concentrated solar power plants. International Journal of Sustainable Energy. 32 (2013) 296-314.